Determinants of Single Photon Response Variability

ALFREDO KIRKWOOD and JOHN E. LISMAN

From the Department of Biology and Center for Complex Systems, Brandeis University, Waltham, Massachusetts 02254

ABSTRACT   The responses to single photon absorptions (quantum bumps) vary randomly in size in *Limulus* photoreceptors. This variability is a natural consequence of simple chemical reactions involving a small number of molecules. The measured size distributions differ significantly from the exponential distribution predicted by the simplest transduction cascade models, one feature of which is that light-activated rhodopsin (R^*) is turned off in a single step process. As shown in the companion paper, the nonexponential size distributions can be accounted for if R^* is turned off in a multi-step process. This would lead to a nonexponential (peaked) distribution in the number of G-protein molecules activated during a quantum bump and to a nonexponential distribution in the size of bumps. To test this possibility we measured the distribution of quantum bump size under two conditions in which the variability in the number of activated G-proteins was eliminated. In one method, bumps were produced by direct activation of single G-proteins using GTP-γ-S; in the second GDP-β-S reduced the R^* gain to the point where most quantal events were due to activation of a single G-protein. In both cases the size distribution of bumps became much closer to an exponential distribution than that of normal light-induced bumps. These results support the idea that the size distribution of light-induced bumps is dependent on events at the R^* level and reflects to the multi-step deactivation of R^*.

INTRODUCTION

Absorption of single photons by *Limulus* photoreceptors produces discrete depolarizing waves (Fuortes and Yeandle, 1964). These single photon responses, termed quantum bumps, are generated by a second messenger cascade that leads to the activation of thousands of ionic channels (Bacigalupo, Chinn, and Lisman, 1986; Wong, 1978). The size of the quantum bump can be quantified by the total charge that flows during the event, and has been found to be highly variable (Grzywacz and Hillman, 1985). This paper concerns the reasons for this variability.

Address correspondence to John E. Lisman, Department of Biology and Center for Complex Systems, Brandeis University, Waltham, MA 02254.

Dr. Kirkwood's present address is Department of Neuroscience, Box 1953, Brown University, Providence, RI 02912.

The companion paper (Goldring and Lisman, 1994), and previous papers (Borsellino and Fuortes, 1968; Grzywacz and Hillman, 1985), argue that a variable response to identical photons is a natural consequence of the stochastic variability inherent in chemical reactions when small numbers of molecules are involved. In the simplest version of a transduction cascade, each active molecule at a given stage activates molecules in the next stage until it gets deactivated in a first-order reaction (Borsellino and Fuortes, 1968). In particular, light-activated rhodopsin (R^*) would activate G-protein molecules until the R^* was deactivated in a one-step reaction (for example, a single phosphorylation reaction). It follows that the lifetime of R^* would be exponentially distributed just as ionic channels with a single open state have an open time that is exponentially distributed. The variability of R^* lifetime and the variability of other reactions in the cascade cause the output of the cascade to be very different from photon to photon. Moreover, analysis of simple cascades indicates that the primary determinant of quantum bump variability is the first stage of amplification where the number of molecules involved is low. Thus, according to this view, quantum bumps variability is strongly dependent on the reactions that control the amplification of the first stage, in particular the reaction(s) that deactivate R^*. As shown in the companion paper (Goldring and Lisman, 1994) and Grzywacz and Hillman, 1985, theory predicts that for the simplest cascade in which R^* is deactivated in a one step reaction, the expected distribution of quantum bump size is exponential.

However, recordings from *Limulus* ventral photoreceptors show that the actual distribution of quantum bump size is often not well fit by an exponential; the distribution may be somewhat peaked at nonzero charge (Lisman and Goldring, 1985; Goldring and Lisman, 1994). This shape can be accounted for if it is assumed that R^* is deactivated in two steps, rather than one. In this case, the distribution of R^* lifetime will have a peaked distribution, as will the number of G-proteins activated and the final cascade output (Lisman and Goldring, 1994).

In this paper we have sought to test the hypothesis that the nonexponential character of the quantum bump size distribution reflects the multi-step deactivation of R^*. We have done so in two independent ways, both of which eliminate the effect that variation in R^* lifetime has on the output of the cascade. If the peakedness of the quantum bump size distribution arises from the peakedness of the distribution of the number of G proteins activated by R^*, quantum bumps activated by a single G protein should not show a peaked distribution. Alternatively, if the peakedness arises from events downstream in the cascade, bypassing the first stage of the cascade should have little effect on the shape of the distribution. Previous work has shown that events generated by activation of single G-proteins are smaller than those generated by photons, but are not so small that they cannot be easily measured (Kirkwood, Weiner, and Lisman 1989). The first method we have used for eliminating the effect of R^* variability was to study the size distribution of quantum bumps generated by the direct activation of G-protein. The second method was to measure the size distribution of light-induced quantum bumps after reducing the R^* gain to the point where most R^* molecules either activated a single G-protein or no G-protein at all. Gain reduction of this kind can be produced by the G-protein inhibitor, GDP-β-S (Kirkwood et al., 1989). Under these low-gain conditions, the

fluctuation in R^* lifetime will not affect the number of G-proteins that contribute to the response because detectable events will be almost exclusively due to the activation of a single G-protein. Our results indicate that under both of these conditions the quantum bump size distribution becomes much closer to an exponential. These results therefore support the hypothesis that the peakedness of the size distribution reflects the multi-step deactivation of R^*.

MATERIALS AND METHODS

Dissection and Recording Procedures

Ventral eyes of *Limulus polyphemus* were removed under bright white light, treated with pronase to ease electrode impalement, and perfused with artificial seawater (ASW) according to standard procedures. The ASW composition was (in mM): 425 NaCl, 10 KCl, 10 $CaCl_2$, 22 $MgCl_2$, 26 $MgSO_4$, 15 Tris-HCl, pH 7.8. The cells were impaled with conventional microelectrodes. The recording electrode was filled with 3 M KCl (10–20 MΩ), while the current electrode was filled with 10 mM GTP-γ-S or 20 mM GDP-β-S, 300 mM KAsp, 10 mM HEPES at pH 7.0 (8–15 MΩ). The Guanosine-nucleotides were injected into the cells by applying brief (30–80 ms) pressure pulses (20–50 psi) to the back of the microelectrode. Pressure injection of drugs was monitored optically with an infra-red video system (Corson and Fein, 1983). GTP-γ-S and GDP-β-S were purchased from Boehringer Mannheim Corp. (Indianapolis, IN).

TABLE I

Cell	Bump rate (bumps/s)			Rejected bumps (percent of total)		
	light$_{before}$	light$_{after}$	GTP-γ-S	light$_{before}$	light$_{after}$	GTP-γ-S
1	1.8	2.8	1.1	25	24	14
2	1.5	3.5	2.2	38	50	31
3	1.9	3.2	2.3	32	51	24
4	0.8	3.9	3.1	20	54	30
5	1.2	2.5	1.1	23	28	20

Data Analysis

Data was acquired at 1 KHz and stored on hard disk. Off line analysis of quantum bumps was done using a BASIC 23 program that detected events with an amplitude at least twice the noise level and an initial slope larger than a threshold (set manually by the experimenter). The size of each quantum bump was calculated by integrating the membrane current over the entire duration of the event. Only isolated quantum bumps were considered for the determination of size distributions; those events in which there was overlap of bumps were ignored. Tables I and II indicate the fraction of bumps rejected because of overlapping for the GTP-γ-S and GDP-β-S experiments, respectively.

The following procedure was used to obtain this distribution of the light induced bumps: histograms were made for the quantum bumps recorded during light and for the spontaneous bumps occurring in the dark (Adolph, 1964). The dark histogram was scaled by the factor (Nl/Nd) (rd/rl), were Nl and Nd are the number of quantum bumps in the light and dark histograms, and rl and rd are the quantum bump rates measured during the light and dark periods. This dark histogram was then subtracted bin by bin from the light histogram to yield the size distribution of the light-induced quantum bumps. This subtraction procedure was not

usually necessary after GDP-β-S injection because the spontaneous quantum bumps virtually disappeared in most cells.

The measured distributions were fit with a single exponential. In doing the fitting we took into consideration that poor fitting might be simply due to the fact that some of the quantum bumps were too small to be detected. To compensate for this, for each experiment a detection limit was defined as the size of the smallest quantum bump recorded. Then the distribution was fit with an exponential only above the detection limit. This was done by subtracting from the smallest bin the expected fraction (U) of undetected bumps (smaller that the detection limit), which was calculated according to: $U = 1 - \exp(-w/A)$, were A is the constant of the exponential (representing the mean bump size) and w is the detection limit. The total area of this compensated exponential distribution was made equal to 1 by multiplying it by $1/(1 - P_s)$, where P_s is the probability that a bump is smaller than the detection limit.

The agreement between the compensated exponential distribution and a measured distribution was quantified by determining the probability (P) that the data could be explained by an exponential. This probability was obtained through an appropriate chi square minimization procedure for finding the best fit for an exponential to the data. The experimental distribution was considered to be the distribution of all the quantum bumps recorded in the light (including

TABLE II

Cell	Bump rate (bumps/s)		Rejected bumps (percent of total)	
	before	after	before	after
1	1.6	1.9	25	15
2	2.0	3.0	27	28
3	1.3	1.6	13	18
4	1.9	2.6	25	30
5	1.5	1.5	12	18
6	1.2	0.9	10	4

Quantum bumps were evoked at similar rates before and after GDP-β-S injection; consequently, the fraction of superimposed bumps did not change substantially after the injection.

spontaneous quantum bumps), and the predicted distribution was considered to be the exponential distribution plus an appropriately weighted distribution of the spontaneous quantum bumps.

RESULTS

Distribution of the Size of the Bumps induced by GTP-γ-S

Previous work has shown that in *Limulus* photoreceptors, intracellular injection of G-protein activators like GTP-γ-S produces discrete waves of depolarization in the dark (Bolsover and Brown, 1982; Corson and Fein, 1983). These waves are similar in time course to the quantum bumps evoked by light, but are, on average, about 10 times smaller, as would be expected if these events are generated downstream in the transduction cascade (Kirkwood et al., 1989). Several lines of additional evidence support the interpretation that these waves arise from activation of G-protein (Kirkwood et al., 1989). Here we have measured the size distribution of the GTP-γ-S-induced bumps and the size distribution of light-induced bumps measured

under the same conditions (i.e., in the presence of GTP-γ-S). Our specific goal was to determine whether the distribution of GTP-γ-S-induced bumps is more closely described by an exponential than the distribution of light-induced bumps.

Before injecting GTP-γ-S, data were collected while the cells were presented with alternating periods of dim light and darkness. Spontaneous bumps occurred in darkness at a low rate ($\sim 1/s$), as previously reported (Adolph, 1964). Sufficient data were collected to measure the size distribution of these events. To determine the size distribution of the light-induced bumps the size of the bumps recorded in the dark was subtracted from the histogram of the bumps recorded during light (see methods). GTP-γ-S was then injected and a bright light stimulus was given to stimulate nucleotide exchange on the G-protein (Bolsover and Brown, 1982). Once the cell dark-adapted, it could be seen that the rate of spontaneous quantum bumps was highly elevated compared to that before injection, as previously described (Bolsover and Brown, 1982). These bumps consisted of GTP-γ-S-induced bumps and normal spontaneous quantum bumps. To obtain the distribution of the GTP-γ-S-induced bumps we first constructed the distribution of the bumps recorded in the dark after the GTP-γ-S injection. From this histogram we subtracted the histogram of the bumps recorded in the dark before the GTP-γ-S injection as described in Materials and Methods; the resulting distribution of GTP-γ-S-induced bumps is shown in Fig. 1 *B*. The cell was then presented with alternating periods of dim light and darkness. To obtain the size distribution of the light-induced quantum bumps we subtracted the size distribution for the bumps recorded in the dark after the GTP-γ-S injection (including spontaneous and GTP-γ-S-induced bumps) from the size distribution of the bumps recorded during light (spontaneous, GTP-γ-S and light-induced bumps). The histogram of light-induced bumps in GTP-γ-S is shown in Fig. 1 *A*.

To determine whether these histograms could be described by an exponential curve, we fit the distributions with an exponential, and determined the adequacy of the fit using chi-square, as described in Materials and Methods. The best fits are shown as the plus signs superposed on the data in Fig. 1 for two cells. It should be noted that the first bin in all histograms shows only bumps larger than the assigned detection limit, which is a significant fraction of the bin width. Thus, for a given exponential distribution, the number of expected observations in the lowest bin was reduced to account for this (see Materials and Methods). The exponential fits in both cells in Fig. 1 are poor ($P < 0.001$) for light-induced bumps. This was true for light-induced bumps both before and after injection (Table III). On the other hand, the fits are quite good for the GTP-γ-S induced bumps ($P > 0.8$ and > 0.3 for cells 1 and 2, respectively). Table III summarizes the results obtained in five experiments. The results in cell 3 were much like those for cells 1 and 2. Thus, for cells 1–3, the distribution of GTP-γ-S-induced bumps appears to be better described by an exponential than the distribution of light-induced bumps. For cells 4 and 5, the size distribution of GTP-γ-S-induced bumps was well fit by an exponential. However, the light-induced bumps after the injection of GTP-γ-S was also reasonably fit by an exponential. Thus no conclusions regarding the basis of the nonexponential distribution can be made from these cells. Goldring and Lisman (1992, unpublished observations) and Grzywacz and Hillman (1985) also have reported instances where the distribution of light-induced bumps can be adequately fit by an exponential.

(A) Light-induced
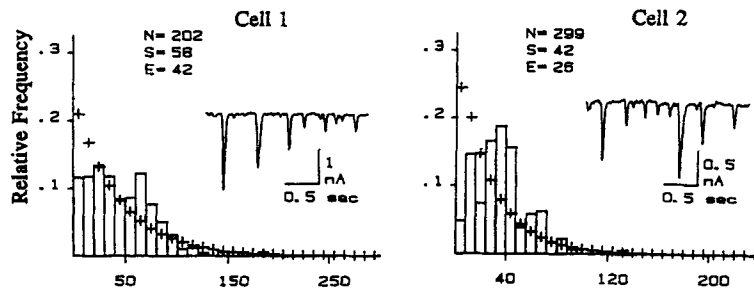
(B) GTP-γ-S-induced
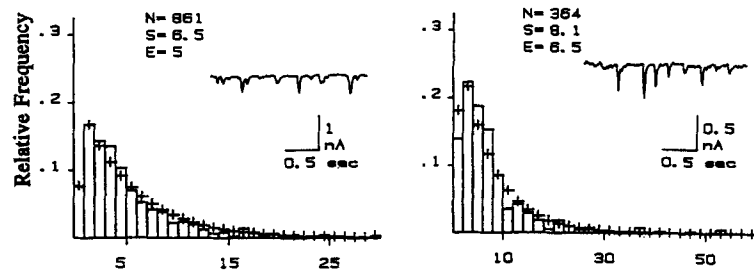
(C) Scaled light-induced
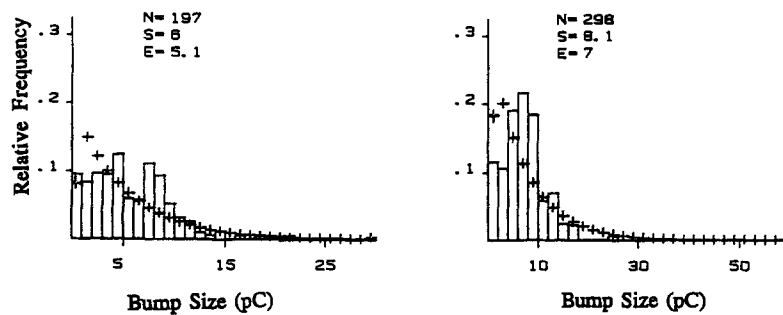

FIGURE 1. Size distribution of the light-induced and GTP-γ-S-induced bumps. Histograms show the size distributions of (A) the light-induced quantum bumps recorded after GTP-γ-S injection and (B) the GTP-γ-S-induced bumps. (C) the distribution of light-induced quantum bumps after they were scaled down to match the size of the GTP-γ-S-induced bumps. The crosses (+) indicate the expected bump frequency according to the exponential that gave the best fit (see Materials and Methods). Insets show examples of the bumps used to compute the distributions. N = number of bumps, S = measured average bump size, E = constant of the exponential that gave the best fit. Data are from cells labeled 1 and 2 in Tables I and III. Bars: 1 s for both cells, 1 nA for cell 1 and 0.5 nA for cell 2.

Because GTP-γ-S-induced bumps are considerably smaller than light-induced bumps we were concerned that the size distribution of GTP-γ-S-induced bumps in cells 1–3 might have the same shape as that of light-induced bumps, only scaled down in size. In this case, the better fit to an exponential might result from the fact that the bumps smaller than the peak of the distribution fell below the detection limit. To check this possibility the light-induced quantum bumps were scaled down to make their average size equal to the average size of GTP-γ-S-induced bumps. All the scaled quantum bumps smaller than the detection limit (defined for each experiment as the smallest quantum bump recorded) were discarded. Then the size distribution for the remaining scaled bumps was determined and its exponential fit evaluated. This scaling test indicates that in none of these three cases could the better agreement with an exponential after GTP-γ-S injection be attributed merely to their smaller size (see Fig. 1 C and Table III). These results therefore support the hypothesis that much of the peakedness of the size distribution of normal light-induced bumps arises from the R^* level of the cascade.

TABLE III

The Size Distribution of GTP-γ-S-Induced Bumps is Closer to an Exponential than the Size Distribution of Light-Induced Quantum Bumps

Cell	$\dfrac{Size_{LIGHT}}{Size_{GTP-\gamma-S}}$	$P_{light\ before}$	$P_{light\ after}$	P_{scaled}	$P_{GTP-\gamma-S}$
1	4.7	$P < 0.005$	$P < 0.001$	$P < 0.001$	$P > 0.80$
2	9.7	$P < 0.005$	$P < 0.001$	$P < 0.001$	$P > 0.30$
3	9.5	$P < 0.005$	$P < 0.001$	$P < 0.001$	$P > 0.30$
4	9.5	$P < 0.005$	$P > 0.20$	$P < 0.01$	$P > 0.30$
5	7.6	$P > 0.75$	$P > 0.70$	$P > 0.80$	$P > 0.30$

The probability that an experimental distribution has an exponential form (see Materials and Methods) is indicated for light-induced quantum bumps before ($P_{light\ before}$) and after injection ($P_{light\ after}$, for GTP-γ-S-induced bumps ($P_{GTP-\gamma-S}$) and for the scaled down (see text) light-induced quantum bumps (P_{scaled}).

Effects of GDP-β-S on the Quantum Bump Size Distribution

Experiments were conducted to determine how intracellular injection of GDP-β-S affects the size distribution of light-induced quantum bumps. Before injection, the size distribution of light induced was measured. GDP-β-S was then injected. As previously described (Kirkwood et al., 1989), GDP-β-S produced a dramatic reduction in the responsiveness of the cell such that it took a much brighter light to generate quantum bumps. The reduction in responsiveness is therefore due to a reduction in quantum efficiency arising from the fact that many R^* molecules never activate even a single unblocked G-protein and thus generate no response. Under these conditions of reduced quantum efficiency, most responses that occur are due to the activation of a single G-protein (Kirkwood et al., 1989). Relative quantum efficiency can be calculated by measuring the probability that an incident photon will evoke a quantum bump. The reduction in quantum efficiency (ΔQE) produced by GDP-β-S for each of the six cells studied is given in Table IV.

The effect of GDP-β-S on the size distribution of light-induced bumps is illustrated in Fig. 2 for two cells. Before the injection, the distributions deviated substantially from an exponential (Fig. 2 A); the distribution for cell 1 has a peak of ~150–240 pC, for cell 2, ~16–32 pC; these distributions could not be fit by an exponential ($P < 0.001$ and $P < 0.05$). In contrast, the size distributions after GDP-β-S injection were much closer to an exponential (Fig. 2 B) ($P > 0.99$ and $P > 0.95$ for cells 1 and 2 respectively). Results on six cells are summarized in Table IV. Before the GDP-β-S injection the size distribution of light-induced bumps substantially deviated from an exponential in all the cases except cell 3. Of the remaining five cells, four became well fit by an exponential after injection.

Again, it was of concern whether the improved fit might be due to the reduction in bump size caused by GDP-β-S. To check this possibility, the scaling test was applied. For cell 2 the light-induced bumps recorded before injection (Fig. 2 C) did not differ

TABLE IV

GDP-β-S Reduces the Disagreement Between the Size Distribution of the Light-Induced Quantum Bumps and an Exponential

Cell	ΔQE	$\dfrac{\text{Size}_{\text{GDP-β-S}}}{\text{Size}_{\text{control}}}$	P_{control}	P_{scaled}	$P_{\text{GDP-β-S}}$
1	4000	0.80	$P < 0.001$	$P < 0.001$	$P > 0.99$
2	16	0.65	$P < 0.05$	$P > 0.10$	$P > 0.95$
3	10	0.37	$P > 0.50$	$P > 0.50$	$P > 0.80$
4	50	0.55	$P < 0.05$	$P < 0.001$	$P > 0.4$
5	4	1.05	$P < 0.001$	$P < 0.001$	$P > 0.3$
6	500	0.80	$P < 0.001$	$P < 0.001$	$P < 0.005$

The relative change in quantum efficiency (ΔQE) after GDP-β-S injection was calculated as previously described (Kirkwood et al., 1989) and is indicated as an n-fold reduction. The probability (according to a X^2 test) that an experimental distribution has an exponential form is indicated for light-induced quantum bumps recorded before the GDP-β-S (P_{control}), for scaled down control quantum bumps (P_{scaled}; see text), and for light-induced quantum bumps recorded after the GDP-β-S injection ($P_{\text{GDP-β-S}}$).

The reader may note that the average size reduction produced by GDP-β-S was only ~20–40%. This reduction is much less than would be expected if the only effect of GDP-β-S were to reduce the first stage gain and probably reflects the fact that this nucleotide also affects adaptation processes which may produce compensatory changes in gain (see Kirkwood et al., 1989).

significantly from an exponential distribution after scaling. Therefore in this cell the better fit to an exponential of light-induced bumps after GDP-β-S might be due to the reduction in bump size. However, in cell 1 (Fig. 2 C, left), cell 4 and cell 5 the distribution deviated significantly from an exponential ($P < 0.05$) even after scaling. In summary, for cells 1, 4, and 5, GDP-β-S changed the distribution from nonexponential to exponential and this change could not be attributed to undetectability of small bumps. On the other hand, cell 6 did not show a closer fit to exponential after injection. No conclusion can be drawn from cell 2 because it failed the scaling test. Thus, in three of the four cells from which conclusions can be drawn, GDP-β-S injection changed the distribution of light-induced bumps from peaked to exponential.
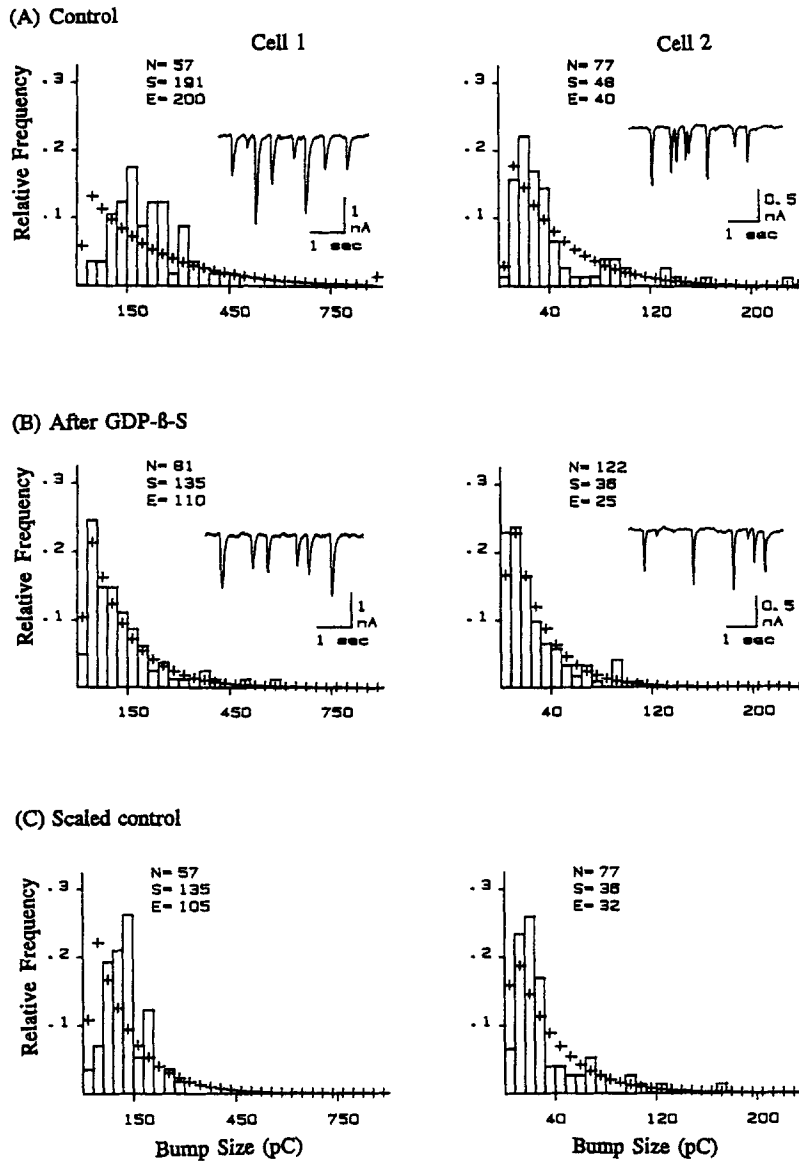
FIGURE 2. Effects of GDP-β-S on the size distribution of the light-induced quantum bumps for two cells (*left and right columns*). The graphs are normalized histograms showing the size (in pC) distribution of the light-induced quantum bumps recorded before (*A*) and after (*B*) injecting GDP-β-S. (*C*) Distribution that results from scaling down the control light-induced quantum bumps (see text). The first bin of the exponential distribution was compensated for the expected number of undetected small bumps (see Materials and Methods). Insets show examples of the quantum bumps used to compute the distributions. After the GDP-β-S injection, the stimulus intensity was increased 4 log units in cell 1 and 1.3 log units in cell 2. Data are from cells labeled 1 and 2 in Table II and IV. Bars: 1 s for both cells, 1 nA for cell 1 and 0.5 nA for cell 2.

DISCUSSION

Our results add to the body of evidence that the size distribution of light-induced quantum bumps, though superficially close to exponential, is usually not exponential (Tables III and IV). In 9 of 11 cells an exponential fit poorly (Tables III and IV). These data, together with those of the companion paper (Goldring and Lisman, 1994) in which quantum bump size distributions were more rigorously measured and analyzed, indicate that the size distribution of light-induced quantum bumps cannot generally be fit by an exponential. The possible causes of the disagreement between our results and those reported by Grzywacz and Hillman (1985) are discussed in the companion paper (Goldring and Lisman, 1994). The main implication of the nonexponential shape of the distribution is that it argues against simple cascade models in which R^* is deactivated in a one step process.

In the companion paper (Goldring and Lisman, 1994) it was shown that the peaked distributions of quantum bump size could be accounted for by simple models in which R^* is deactivated in two steps. The goal of this paper has been to test this hypothesis by studying conditions in which the kinetics of R^* deactivation has no effect on the quantum bump size distribution. Two conditions under which only one G-protein contributes to the response have been studied. In the first, GTP-γ-S was injected to directly activate G-protein molecules. Here what is compared are the bumps evoked in the dark by this nucleotide to those evoked by light under the same conditions. The bumps evoked by GTP-γ-S were much closer to an exponential distribution than those evoked by light under the same conditions. In a second test, GDP-β-S was used to reduce the average first stage gain to such a low value that most observed responses were due to activation of a single G-protein. Under these conditions the size distribution of light-induced quantum bumps was closer to exponential than before nucleotide injection. Taken together, these results therefore suggest that the deviation from exponentiality is due in large part to events at the first stage of transduction. Additional contributions from subsequent stages of the cascade cannot be ruled out.

One objection to this conclusion stems from the fact that both methods we have used bypass the first stage gain, making it possible that the change in shape of the area distributions is a secondary consequence of gain reduction. In particular, suppose that the normal high gain leads to saturation of a step in the cascade and that lowering gain prevents this saturation. Because saturation produces peakedness in the size distribution, reducing gain might prevent saturation and thereby diminish peakedness. This possibility seems unlikely because in some cells (1 and 5 in Table IV) GDP-β-S reduced peakedness without substantially affecting overall gain (probably because some downstream gain increase compensates for the reduction in number of G-proteins activated). Thus, it is difficult to see how the reduction in peakedness after GDP-β-S could be attributed to a saturation effect.

The biochemistry underlying the deactivation of invertebrate visual pigment has not yet been completely worked out. It is known that rhodopsin is phosphorylated after illumination (Vandenberg and Montal, 1984), that deactivation is dependent on soluble factors and on ATP (Kahana, Robinson, Lewis, Szuts, and Lisman, 1992), that invertebrates have homologs of vertebrate arrestin (Smith, Shieh, and Zucker, 1990)

and that arrestin is involved in deactivation (Dolph et al., 1993). These findings are generally consistent with those found in vertebrate photoreceptors where rhodopsin deactivation is clearly a multi-step process, involving rhodopsin phosphorylation (Sitaramayya and Liebman, 1983; Wilden and Khun; 1982) followed by arrestin binding (Kuhn, Hall, and Wilden, 1984). Our conclusion that deactivation of *Limulus* rhodopsin is a multi-step process would thus appear reasonable in light of what is known biochemically about deactivation of vertebrate rhodopsin.

Our ability to influence the variability of the cascade output using pharmacological agents that affect an early step in transduction supports the idea that the stochastic fluctuation of single photon events provides the electrophysiologist with a way of studying the initial steps in transduction. It may be thought that early steps in the cascade could not be studied through examination of the output of the cascade, many steps removed from rhodopsin. However, the stochastic aspects of single photon events are determined when the number of molecules involved is small and it is for this reason that early steps in the cascade have such a powerful effect on the viability of the output. Studies of output variability thus provide information about the initial steps of transduction in living cells that nicely complements other methods that are becoming available for studying rhodopsin deactivation in living cells (Richard and Lisman, 1992).

REFERENCES

Adolph, A. R. 1964. Spontaneous potential fluctuations in the *Limulus* photoreceptor. *Journal of General Physiology.* 48:297–321.

Bacigalupo, J., K. Chinn, and J. Lisman. 1986. Ion channels activated by light in *Limulus* ventral photoreceptors. *Journal of General Physiology.* 87:73–89.

Bolsover, S. R., and J. E. Brown. 1982. Injection of guanosine and adenosine nucleotides into *Limulus* ventral photoreceptor cells. *Journal of Physiology.* 332:325–342.

Borsellino, A., and M. G. F. Fuortes. 1968. Responses to single photons in visual cells of *Limulus*. *Journal of Physiology.* 196:507–539.

Corson, W., and A. Fein. 1983. Chemical excitation of *Limulus* photoreceptors. Phosphatase inhibitors induce discrete-wave production in the dark. *Journal of General Physiology.* 82:639–657.

Dolph, P. J., R. Ranganathan, N. J. Colley, R. W. Hardy, M. Socolich, and C. S. Zukee. 1993. Arrestin function in inactivation of G protein-coupled receptor rhodopsin in vivo. *Science.* 260:1910–1916.

Fuortes, M. G. F., and S. Yeandle. 1964. Probability of occurrence of discrete potential waves in cells of the eye of *Limulus*. *Journal of General Physiology.* 46:443–463.

Goldring, M., and J. E. Lisman. 1994. Multi-step rhodopsin inactivation can account for the size variability of single photon responses in *Limulus* ventral photoreceptors. *Journal of General Physiology.* 103:691–727.

Grzywacz, N. M., and P. Hillman. 1985. Statistical test of linearity of phototransduction process: *Limulus* passes, others fails. *Proceedings of the National Academy of Sciences, USA.* 82:232–235.

Kahana, A., P. R. Robinson, L. J. Lewis, E. Z. Szuts, and J. E. Lisman. 1992. ATP-independent deactivation of squid rhodopsin. *Visual Neuroscience.* 9:595–602.

Kirkwood, A., D. Weiner, and J. E. Lisman. 1989. An estimate of the number of G regulatory proteins activated per excited rhodopsin in living *Limulus* ventral photoreceptors. *Proceedings of the National Academy of Sciences USA.* 86:3872–3876.

Khun, H. S. W. Hall, and U. Wilden. 1984. Light-induced binding of 48-kD protein to photoreceptor membranes is highly enhanced by phosphorylation of rhodopsin. *FEBS Letters.* 176:473–478.

Lisman, J., and M. Goldring. 1985. Early events in visual transduction in *Limulus* photoreceptors. *Neuroscience Research Supplement.* 2:101–117.

Richard, E. A., and J. E. Lisman. 1992. Rhodopsin inactivation is a modulated process in *Limulus* photoreceptors. *Nature.* In press.

Smith, D. P., B. Shieh, and C. S. Zucker. 1990. Isolation and structure of an arrestin gene from *Drosophila. Proceedings of the National Academy of Sciences, USA.* 87:1003–1007.

Sitaramayya, A., and P. A. Liebman. 1983. Phosphorylation of rhodopsin and quenching of cyclic GMP phosphodiesterase by ATP at weak bleaches. *Journal of Biological Chemistry.* 258:12106–12109.

Vandenberg, C. A., and M. Montal. 1984. Light-regulated biochemical events in invertebrate photoreceptors. II. Light-regulated phosphorylation of rhodopsin and phosphoinositides in squid photoreceptor membranes. *Biochemistry.* 23:2347–2352.

Wilden, U., and H. Kuhn. 1982. Light-dependent phosphorylation of rhodopsin: number of phosphorylation sites. *Biochemistry.* 21:3014–3022.

Wong, F. 1978. Nature of light-induced conductance changes in ventral photoreceptors of *Limulus. Nature.* 276:76–79.